Generalized Hanbury Brown–Twiss effect in partially coherent electromagnetic beams

Gaofeng Wu
School of Physics, Northwest University, Xian 710069, China

David Kuebel
Department of Physics and Astronomy, University of Rochester, Rochester, New York 14627, USA and St. John Fisher College, Rochester, New York 14618, USA

Taco D. Visser
Department of Physics and Astronomy, Vrije Universiteit, Amsterdam, NL-1081HV, The Netherlands and Department of Physics and Astronomy, University of Rochester, Rochester, New York 14627, USA

(Received 14 January 2019; published 25 March 2019)

The recently introduced concept of Stokes fluctuations generalizes both the Hanbury Brown–Twiss effect and the notion of scintillation. Here we apply this new framework to the specific example of a Gaussian Schell-model (GSM) beam. We derive formulas for Stokes scintillations and Stokes fluctuation correlations, which explicitly express the dependence of these quantities on the GSM source parameters. It is found that the normalized Stokes scintillations vary significantly with position. Also, they can be either positively or negatively correlated.

DOI: 10.1103/PhysRevA.99.033846

I. INTRODUCTION

Recent work on intensity correlations has attempted to extend the study of the Hanbury Brown–Twiss (HBT) effect [1–3], as customarily applied to fields of research such as astronomy and quantum optics, to the case of vector electromagnetic beams. One avenue of investigation on this topic is to explore the possible relationship between the state of polarization of the beam and the behavior of the observable HBT coefficient. Such calculations have been presented in Refs. [4–9]. In considering the polarization-resolved HBT effect it seems natural to employ the traditional Stokes parameters to describe the state of polarization of the beam. In fact, it is trivial to observe that the HBT coefficient itself can also be expressed in terms of the first Stokes parameter, denoted by S_0. The correlation of the intensity fluctuations can therefore be thought of as a quantity that is directly related to the polarization state. Recently this observation was generalized by defining the complete class of Stokes fluctuation correlations [10]. Similarly, the scintillation coefficient, which is nothing but the local variance of S_0, can be generalized to a class of one-point correlations between the various Stokes parameters. We refer to these generalized quantities as Stokes fluctuation correlations and Stokes scintillations, respectively. Under the assumption of Gaussian statistics, a single expression for all these quantities can be derived. In this paper we apply the formalism that describes a generalized HBT experiment to a broad class of partially coherent beams, namely those of the Gaussian Schell-model type. We study how the Stokes fluctuation correlations and Stokes scintillations in the far zone are affected by the source parameters. Both these quantities are found to display a rich behavior. For example, the normalized Stokes scintillations vary strongly with position, and their correlations can either be positive or negative.

A sketch for a generalized, polarization-resolved HBT experiment that could be used to measure the quantities of interest described in this paper is shown in Fig. 1. The field that is incident on the two detectors is spectrally filtered and passed through polarizing elements. The elements are chosen such that each detector measures a particular spectral Stokes parameter. In a traditional HBT experiment these filters and polarizers would be absent.

II. STOKES FLUCTUATION CORRELATIONS AND STOKES SCINTILLATIONS

The second-order statistical properties of a partially coherent electromagnetic beam are described by its cross-spectral density matrix, which is defined as [11]

$$\mathbf{W}(\mathbf{r}_1, \mathbf{r}_2, \omega) = \begin{pmatrix} W_{xx} & W_{xy} \\ W_{yx} & W_{yy} \end{pmatrix}. \tag{1}$$

All the matrix elements are functions of the same three variables, and given by the expression

$$W_{ij}(\mathbf{r}_1, \mathbf{r}_2, \omega) = \langle E_i^*(\mathbf{r}_1, \omega) E_j(\mathbf{r}_2, \omega)\rangle, \quad (i, j = x, y), \tag{2}$$

where $\mathbf{r}_1$ and $\mathbf{r}_2$ are two points of observation, ω is the angular frequency, and the angular brackets indicate an average taken over an ensemble of beam realizations.

The state of polarization of the beam is described by the four Stokes parameters [12]. Their average value can be expressed in terms of the cross-spectral density matrix evaluated at $\mathbf{r}_1 = \mathbf{r}_2 = \mathbf{r}$ as

$$\langle S_0(\mathbf{r}, \omega)\rangle = W_{xx}(\mathbf{r}, \mathbf{r}, \omega) + W_{yy}(\mathbf{r}, \mathbf{r}, \omega), \tag{3a}$$

$$\langle S_1(\mathbf{r}, \omega)\rangle = W_{xx}(\mathbf{r}, \mathbf{r}, \omega) - W_{yy}(\mathbf{r}, \mathbf{r}, \omega), \tag{3b}$$

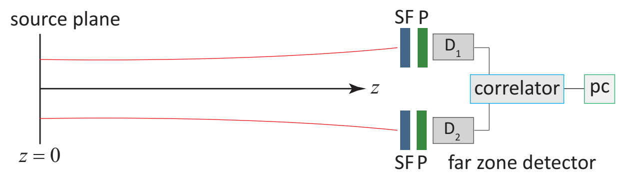

FIG. 1. A polarization-resolved HBT experiment. The far-zone radiation of a source is passed through a narrow-band spectral filter (SF) and polarizing elements (P) that cover two intensity detectors D_1 and D_2. The output of the detectors is correlated and sent to a computer (pc).

$$\langle S_2(\mathbf{r}, \omega)\rangle = W_{xy}(\mathbf{r}, \mathbf{r}, \omega) + W_{yx}(\mathbf{r}, \mathbf{r}, \omega), \tag{3c}$$

$$\langle S_3(\mathbf{r}, \omega)\rangle = \mathrm{i}[W_{yx}(\mathbf{r}, \mathbf{r}, \omega) - W_{xy}(\mathbf{r}, \mathbf{r}, \omega)]. \tag{3d}$$

All preceding equations have an explicit frequency dependence, indicating that they are defined for a specific frequency component of the optical field. For brevity, we will no longer display this ω dependence from now on.

For the case of a stochastic beam the Stokes parameters are not deterministic, but they are random quantities. The fluctuations around their average value (i.e., the Stokes fluctuations) are defined as

$$\Delta S_n(\mathbf{r}) = S_n(\mathbf{r}) - \langle S_n(\mathbf{r})\rangle \quad (n = 0, 1, 2, 3), \tag{4}$$

where $S_n(\mathbf{r})$ is the Stokes parameter pertaining to a single realization of the beam, and $\langle S_n(\mathbf{r})\rangle$ denotes its ensemble average. We can now examine how these Stokes fluctuations are correlated. All possible pairs of their two-point correlations can be captured by introducing a 4×4 Stokes fluctuation correlation matrix $\mathbf{C}(\mathbf{r}_1, \mathbf{r}_2)$, whose elements are

$$C_{nm}(\mathbf{r}_1, \mathbf{r}_2) \equiv \langle \Delta S_n(\mathbf{r}_1)\Delta S_m(\mathbf{r}_2)\rangle \quad (n, m = 0, 1, 2, 3). \tag{5}$$

We recently showed, under the assumption that the source that generates the beam is governed by Gaussian statistics, that these elements can be expressed as [10]

$$C_{nm}(\mathbf{r}_1, \mathbf{r}_2) = \sum_{a,b}\sum_{c,d} \sigma^n_{ab}\sigma^m_{cd} W_{ad}(\mathbf{r}_1, \mathbf{r}_2) W^*_{bc}(\mathbf{r}_1, \mathbf{r}_2),$$
$$(a, b, c, d = x, y), \tag{6}$$

where $\boldsymbol{\sigma}^0$ denotes the 2×2 identity matrix, and the Pauli spin matrices are defined as

$$\boldsymbol{\sigma}^1 = \begin{pmatrix} 1 & 0 \\ 0 & -1 \end{pmatrix}, \quad \boldsymbol{\sigma}^2 = \begin{pmatrix} 0 & 1 \\ 1 & 0 \end{pmatrix}, \quad \boldsymbol{\sigma}^3 = \begin{pmatrix} 0 & -\mathrm{i} \\ \mathrm{i} & 0 \end{pmatrix}, \tag{7}$$

respectively. We remind the reader that, in contrast to the Stokes fluctuations whose correlations are described by Eq. (6), the Stokes parameters themselves are related by the inequality [12]

$$\langle S_0^2(\mathbf{r})\rangle \geqslant \langle S_1^2(\mathbf{r})\rangle + \langle S_2^2(\mathbf{r})\rangle + \langle S_3^2(\mathbf{r})\rangle, \tag{8}$$

with the equal sign holding only for a fully polarized beam.

Working out Eq. (6) for all sixteen elements results in

$$C_{00}(\mathbf{r}_1, \mathbf{r}_2) = |W_{xx}|^2 + |W_{xy}|^2 + |W_{yx}|^2 + |W_{yy}|^2, \tag{9a}$$

$$C_{01}(\mathbf{r}_1, \mathbf{r}_2) = |W_{xx}|^2 - |W_{xy}|^2 + |W_{yx}|^2 - |W_{yy}|^2, \tag{9b}$$

$$C_{02}(\mathbf{r}_1, \mathbf{r}_2) = 2\,\mathrm{Re}\,[W_{xx}W^*_{xy} + W_{yy}W^*_{yx}], \tag{9c}$$

$$C_{03}(\mathbf{r}_1, \mathbf{r}_2) = 2\,\mathrm{Im}\,[W_{yy}W^*_{yx} - W_{xx}W^*_{xy}], \tag{9d}$$

$$C_{10}(\mathbf{r}_1, \mathbf{r}_2) = |W_{xx}|^2 + |W_{xy}|^2 - |W_{yx}|^2 - |W_{yy}|^2, \tag{9e}$$

$$C_{11}(\mathbf{r}_1, \mathbf{r}_2) = |W_{xx}|^2 - |W_{xy}|^2 - |W_{yx}|^2 + |W_{yy}|^2, \tag{9f}$$

$$C_{12}(\mathbf{r}_1, \mathbf{r}_2) = 2\,\mathrm{Re}\,[W_{xx}W^*_{xy} - W_{yy}W^*_{yx}], \tag{9g}$$

$$C_{13}(\mathbf{r}_1, \mathbf{r}_2) = 2\,\mathrm{Im}\,[W_{xy}W^*_{xx} + W_{yx}W^*_{yy}], \tag{9h}$$

$$C_{20}(\mathbf{r}_1, \mathbf{r}_2) = 2\,\mathrm{Re}\,[W_{xx}W^*_{yx} + W_{yy}W^*_{xy}], \tag{9i}$$

$$C_{21}(\mathbf{r}_1, \mathbf{r}_2) = 2\,\mathrm{Re}\,[W_{xx}W^*_{yx} - W_{yy}W^*_{xy}], \tag{9j}$$

$$C_{22}(\mathbf{r}_1, \mathbf{r}_2) = 2\,\mathrm{Re}\,[W_{xx}W^*_{yy} + W_{xy}W^*_{yx}], \tag{9k}$$

$$C_{23}(\mathbf{r}_1, \mathbf{r}_2) = 2\,\mathrm{Im}\,[W_{xy}W^*_{yx} + W^*_{xx}W_{yy}], \tag{9l}$$

$$C_{30}(\mathbf{r}_1, \mathbf{r}_2) = 2\,\mathrm{Im}\,[W_{xx}W^*_{yx} - W_{yy}W^*_{xy}], \tag{9m}$$

$$C_{31}(\mathbf{r}_1, \mathbf{r}_2) = 2\,\mathrm{Im}\,[W_{xx}W^*_{yx} + W_{yy}W^*_{xy}], \tag{9n}$$

$$C_{32}(\mathbf{r}_1, \mathbf{r}_2) = 2\,\mathrm{Im}\,[W_{xy}W^*_{yx} + W_{xx}W^*_{yy}], \tag{9o}$$

$$C_{33}(\mathbf{r}_1, \mathbf{r}_2) = 2\,\mathrm{Re}\,[W_{xx}W^*_{yy} - W_{xy}W^*_{yx}], \tag{9p}$$

where on the right-hand side the $(\mathbf{r}_1, \mathbf{r}_2)$ dependence of the cross-spectral density matrix elements W_{ij} has been suppressed for brevity. It is seen that, in the general case, all elements $C_{nm}(\mathbf{r}_1, \mathbf{r}_2)$ are nonzero. This means that the fluctuations of any Stokes parameter at a position $\mathbf{r}_1$ are correlated with the fluctuations of all four Stokes parameters at another position $\mathbf{r}_2$. As a partial check it can be verified that the expression for the first matrix element, $C_{00}(\mathbf{r}_1, \mathbf{r}_2)$, is indeed equivalent to that of the usual Hanbury Brown–Twiss coefficient [4].

When the two spatial arguments of $C_{nm}(\mathbf{r}_1, \mathbf{r}_2)$ coincide, it reduces to the Stokes scintillation matrix $D_{nm}(\mathbf{r})$, i.e.,

$$D_{nm}(\mathbf{r}) \equiv C_{nm}(\mathbf{r}, \mathbf{r}). \tag{10}$$

We note that the $D_{00}(\mathbf{r})$ element represents the usual scintillation coefficient. It can be derived that [10]

$$D_{00}(\mathbf{r}) = \tfrac{1}{2}[\langle S_0(\mathbf{r})\rangle^2 + \langle S_1(\mathbf{r})\rangle^2 + \langle S_2(\mathbf{r})\rangle^2 + \langle S_3(\mathbf{r})\rangle^2], \tag{11a}$$

$$D_{11}(\mathbf{r}) = \tfrac{1}{2}[(\langle S_0(\mathbf{r})\rangle^2 + \langle S_1(\mathbf{r})\rangle^2 - \langle S_2(\mathbf{r})\rangle^2 - \langle S_3(\mathbf{r})\rangle^2], \tag{11b}$$

$$D_{22}(\mathbf{r}) = \tfrac{1}{2}[\langle S_0(\mathbf{r})\rangle^2 - \langle S_1(\mathbf{r})\rangle^2 + \langle S_2(\mathbf{r})\rangle^2 - \langle S_3(\mathbf{r})\rangle^2], \tag{11c}$$

$$D_{33}(\mathbf{r}) = \tfrac{1}{2}[\langle S_0(\mathbf{r})\rangle^2 - \langle S_1(\mathbf{r})\rangle^2 - \langle S_2(\mathbf{r})\rangle^2 + \langle S_3(\mathbf{r})\rangle^2]. \tag{11d}$$

From these expressions it is seen that $D_{00}(\mathbf{r})$ is greater than or equal to the other three diagonal elements. The twelve off-diagonal elements are given by the expressions

$$D_{pq}(\mathbf{r}) = \langle S_p(\mathbf{r})\rangle\langle S_q(\mathbf{r})\rangle, \quad (p \neq q;\ \text{and}\ p, q = 0, 1, 2, 3). \tag{12}$$

It is useful to introduce a normalized version of the two correlation matrices, indicated by the superscript N, by defining

$$C^N_{nm}(\mathbf{r}_1, \mathbf{r}_2) = \frac{C_{nm}(\mathbf{r}_1, \mathbf{r}_2)}{\langle S_0(\mathbf{r}_1)\rangle\langle S_0(\mathbf{r}_2)\rangle}, \tag{13}$$

and

$$D_{nm}^N(\mathbf{r}) = \frac{D_{nm}(\mathbf{r})}{\langle S_0(\mathbf{r})\rangle^2}. \tag{14}$$

The sum of the four diagonal elements of the $\mathbf{C}^N(\mathbf{r}_1, \mathbf{r}_2)$ matrix has a distinct physical meaning [10], namely

$$\sum_{m=0}^{3} C_{mm}^N(\mathbf{r}_1, \mathbf{r}_2) = 2|\eta(\mathbf{r}_1, \mathbf{r}_2)|^2. \tag{15}$$

Here $\eta(\mathbf{r}_1, \mathbf{r}_2)$ denotes the spectral degree of coherence [11], the magnitude of which indicates the visibility of the interference pattern produced in Young's experiment with pinholes located at $\mathbf{r}_1$ and $\mathbf{r}_2$. Similarly, the sum of the four normalized diagonal Stokes scintillations satisfies the relation

$$\sum_{m=0}^{3} D_{mm}^N(\mathbf{r}) = 2. \tag{16}$$

The element $D_{00}^N(\mathbf{r})$ is equal to the square of the scintillation index [13], and is bounded, namely [14]

$$\frac{1}{2} \leqslant D_{00}^N(\mathbf{r}) \leqslant 1. \tag{17}$$

It follows from Eqs. (12) and (14) that the off-diagonal elements of the $\mathbf{D}^N(\mathbf{r})$ matrix are also not independent. For example, $D_{23}^N(\mathbf{r}) = D_{02}^N(\mathbf{r})D_{03}^N(\mathbf{r})$. In the next section we calculate the Stokes fluctuation correlations and the Stokes scintillations that occur in a specific type of beam.

III. GAUSSIAN SCHELL-MODEL BEAMS

The cross-spectral density matrix elements of an electromagnetic Gaussian Schell-model (GSM) beam in its source plane, indicated by the superscript (0), are [11]

$$W_{ij}^{(0)}(\boldsymbol{\rho}_1, \boldsymbol{\rho}_2) = A_i A_j B_{ij} \exp\left[-\frac{\rho_1^2}{4\sigma_i^2} - \frac{\rho_2^2}{4\sigma_j^2} - \frac{(\boldsymbol{\rho}_1 - \boldsymbol{\rho}_2)^2}{2\delta_{ij}^2}\right],$$
$$(i, j = x, y). \tag{18}$$

The parameters $A_i, B_{ij}, \sigma_i, \delta_{ij}$ are independent of position, but may depend on frequency. They can not be chosen freely, but have to satisfy several constraints, i.e.,

$$B_{xx} = B_{yy} = 1, \tag{19}$$

$$B_{xy} = B_{yx}^*, \tag{20}$$

$$B_{xy} = |B_{xy}|e^{i\phi}, \text{ with } |B_{xy}| \leqslant 1, \text{ and } \phi \in \mathbb{R}, \tag{21}$$

$$\delta_{xy} = \delta_{yx}. \tag{22}$$

Furthermore, the so-called realizability conditions are [15]

$$\sqrt{\frac{\delta_{xx}^2 + \delta_{yy}^2}{2}} \leqslant \delta_{xy} \leqslant \sqrt{\frac{\delta_{xx}\delta_{yy}}{|B_{xy}|}}. \tag{23}$$

For the case $\sigma_x = \sigma_y = \sigma$, the source will generate a beamlike field if [16]

$$\frac{1}{4\sigma^2} + \frac{1}{\delta_{xx}^2} \ll \frac{2\pi^2}{\lambda^2}, \quad \text{and} \quad \frac{1}{4\sigma^2} + \frac{1}{\delta_{yy}^2} \ll \frac{2\pi^2}{\lambda^2}, \tag{24}$$

where λ denotes the wavelength. On propagation to a transverse plane z the matrix elements evolve into [11]

$$W_{ij}(\boldsymbol{\rho}_1, \boldsymbol{\rho}_2, z) = \frac{A_i A_j B_{ij}}{\Delta_{ij}^2(z)} \exp\left[-\frac{(\boldsymbol{\rho}_1 + \boldsymbol{\rho}_2)^2}{8\sigma^2\Delta_{ij}^2(z)}\right]$$
$$\times \exp\left[-\frac{(\boldsymbol{\rho}_1 - \boldsymbol{\rho}_2)^2}{2\Omega_{ij}^2\Delta_{ij}^2(z)} + \frac{ik(\rho_2^2 - \rho_1^2)}{2R_{ij}(z)}\right], \tag{25}$$

where

$$\Delta_{ij}^2(z) = 1 + (z/\sigma k\Omega_{ij})^2, \tag{26}$$

$$\frac{1}{\Omega_{ij}^2} = \frac{1}{4\sigma^2} + \frac{1}{\delta_{ij}^2}, \tag{27}$$

$$R_{ij}(z) = [1 + (\sigma k\Omega_{ij}/z)^2]z. \tag{28}$$

When z tends to infinity we have

$$\Delta_{ij}^2(z) \sim \frac{z^2}{(\sigma k\Omega_{ij})^2}, \tag{29}$$

$$R_{ij}(z) \sim z. \tag{30}$$

We thus get for the far-zone elements, denoted by the superscript (∞), the expressions

$$W_{ij}^{(\infty)}(\boldsymbol{\rho}_1, \boldsymbol{\rho}_2, z)$$
$$= \frac{A_i A_j B_{ij}(k\sigma\Omega_{ij})^2}{z^2} \exp\left[-\frac{(\boldsymbol{\rho}_1 + \boldsymbol{\rho}_2)^2(k\Omega_{ij})^2}{8z^2}\right]$$
$$\times \exp\left[-\frac{(\boldsymbol{\rho}_1 - \boldsymbol{\rho}_2)^2(k\sigma)^2}{2z^2} + \frac{ik(\rho_2^2 - \rho_1^2)}{2z}\right]. \tag{31}$$

Let us assume, for simplicity, that the amplitude of the two spectral densities and the two autocorrelation radii are the same, i.e.,

$$A_x = A_y = A, \tag{32}$$

$$\delta_{xx} = \delta_{yy} = \delta. \tag{33}$$

This implies that

$$\Omega_{xx} = \Omega_{yy} = \Omega. \tag{34}$$

In the far zone the observation points are given by the polar angle $\theta \approx \tan\theta = \rho/z$, the azimuthal angle is not needed. Hence we can write

$$W_{ij}^{(\infty)}(\theta, \theta, z) = K^2 B_{ij}\Omega_{ij}^2 e^{-\theta^2k^2\Omega_{ij}^2/2}, \tag{35}$$

$$W_{ij}^{(\infty)}(0, \theta, z) = K^2 B_{ij}\Omega_{ij}^2 e^{-\theta^2k^2\Omega_{ij}^2/8} e^{-\theta^2k^2\sigma^2/2} e^{ik\theta^2z/2}, \tag{36}$$

where

$$K^2 = \left(\frac{Ak\sigma}{z}\right)^2. \tag{37}$$

We will use these two expressions to study the far-zone scintillations and the far-zone fluctuation correlations.

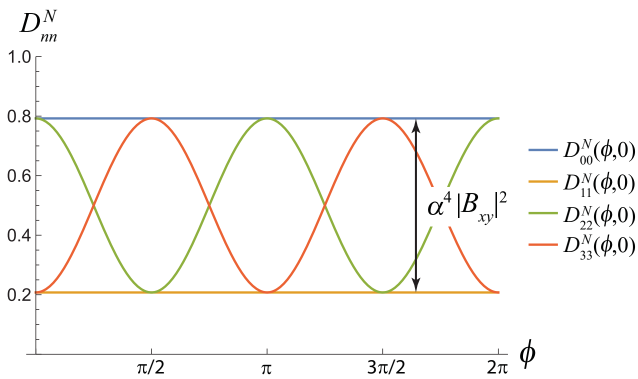

FIG. 2. The four diagonal Stokes scintillations on the far-zone axis ($\theta = 0$) as a function of the argument ϕ of the coefficient B_{xy}. In this example $\lambda = 632.8$ nm, $\sigma = 1$ cm, $\delta = 4$ mm, $\delta_{xy} = 5$ mm, and $|B_{xy}| = 0.5$. The upper straight curve is for $D^N_{00}(\phi, 0)$, the lower one is for $D^N_{11}(\phi, 0)$. Of the two oscillating curves the upper one at $\phi = 0$ corresponds to $D^N_{22}(\phi, 0)$, the lower one to $D^N_{33}(\phi, 0)$.

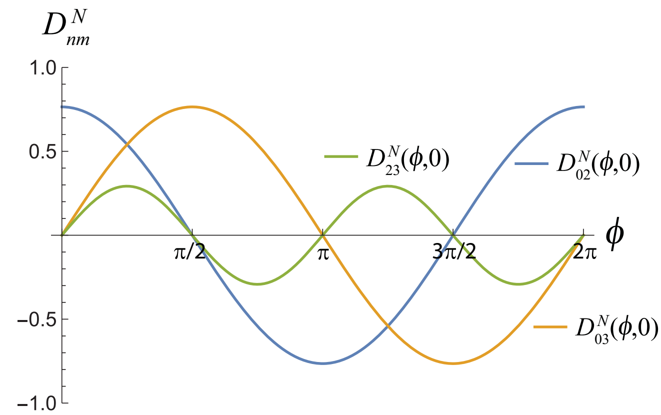

FIG. 3. The nonzero off-diagonal Stokes scintillations on the far-zone axis as a function of the argument ϕ of the coefficient B_{xy}. The parameters are the same as in Fig. 2.

IV. STOKES SCINTILLATIONS

On substituting from Eq. (35) into Eq. (14), while making use of Eqs. (9a)–(9p), we find for the four diagonal far-zone normalized Stokes scintillations that

$$D^N_{00}(\theta) = \tfrac{1}{2}[1 + \alpha^4|B_{xy}|^2 e^{-\theta^2k^2(\Omega^2_{xy}-\Omega^2)}], \tag{38a}$$

$$D^N_{11}(\theta) = \tfrac{1}{2}[1 - \alpha^4|B_{xy}|^2 e^{-\theta^2k^2(\Omega^2_{xy}-\Omega^2)}], \tag{38b}$$

$$D^N_{22}(\theta) = \tfrac{1}{2}[1 + \alpha^4|B_{xy}|^2 \cos(2\phi) e^{-\theta^2k^2(\Omega^2_{xy}-\Omega^2)}], \tag{38c}$$

$$D^N_{33}(\theta) = \tfrac{1}{2}[1 - \alpha^4|B_{xy}|^2 \cos(2\phi) e^{-\theta^2k^2(\Omega^2_{xy}-\Omega^2)}], \tag{38d}$$

where $\alpha \equiv \Omega_{xy}/\Omega \geqslant 1$. This inequality is a direct consequence of the realizability conditions Eq. (23). It implies that the exponential functions in Eqs. (38a)–(38d) all decrease with increasing θ. An example of how the on-axis Stokes scintillations may behave is presented in Fig. 2. There the four diagonal scintillation coefficients are plotted as a function of ϕ, the argument of the complex coefficient B_{xy} which is defined in Eq. (18). Note that ϕ is the expectation value of the phase difference between E_x and E_y. The first two coefficients, D_{00} (which is the usual scintillation coefficient) and D_{11}, are independent of ϕ whereas the other two coefficients display a harmonic behavior. This can be understood as follows: the scintillations of S_0 and S_1 are, according to their definitions, only dependent on the fluctuations of $|E_x|^2$ and $|E_y|^2$ and are therefore independent of the angle ϕ. Since the other two Stokes parameters, S_2 and S_3, contain cross terms of E_x and E_y, their scintillations do depend on ϕ. Notice that although the individual Stokes scintillations may vary, their sum remains constant at two, in agreement with Eq. (16).

The off-diagonal scintillations can be expressed in terms of the average of the Stokes parameters, as indicated by Eq. (12). Using Eqs. (3a)–(3d) and (35) we find that

$$S^{(\infty)}_0(\theta) = 2K^2\Omega^2 \exp\left(-\frac{k^2\Omega^2\theta^2}{2}\right), \tag{39a}$$

$$S^{(\infty)}_1(\theta) = 0, \tag{39b}$$

$$S^{(\infty)}_2(\theta) = 2K^2\Omega^2_{xy}|B_{xy}| \cos\phi \exp\left(-\frac{k^2\Omega^2_{xy}\theta^2}{2}\right), \tag{39c}$$

$$S^{(\infty)}_3(\theta) = 2K^2\Omega^2_{xy}|B_{xy}| \sin\phi \exp\left(-\frac{k^2\Omega^2_{xy}\theta^2}{2}\right). \tag{39d}$$

Hence the six nonzero off-diagonal scintillation coefficients are

$$D^N_{02}(\theta) = D^N_{20}(\theta) = \alpha^2|B_{xy}| \cos\phi \exp\left[-\frac{\theta^2k^2}{2}(\Omega^2_{xy} - \Omega^2)\right], \tag{40a}$$

$$D^N_{03}(\theta) = D^N_{30}(\theta) = \alpha^2|B_{xy}| \sin\phi \exp\left[-\frac{\theta^2k^2}{2}(\Omega^2_{xy} - \Omega^2)\right], \tag{40b}$$

$$D^N_{23}(\theta) = D^N_{32}(\theta) = \alpha^4|B_{xy}|^2 \cos\phi \sin\phi \exp\left[-\theta^2k^2(\Omega^2_{xy} - \Omega^2)\right]. \tag{40c}$$

An example is shown in Fig. 3. The behavior is quite distinct from that of the diagonal scintillation coefficients. Whereas for our model choice the diagonal elements are always positive, the off-diagonal scintillation coefficients can also attain negative values.

It is seen from Eqs. (40a)–(40c) that the off-diagonal Stokes scintillations, unlike their diagonal counterparts, do not all have the same exponential dependence on the angle of observation θ. This is illustrated in Fig. 4. When θ gets larger, all scintillation coefficients tend to zero, but they do so from different initial, on-axis values.

V. STOKES FLUCTUATION CORRELATIONS

For the far-zone field we can use Eqs. (35) and (36) to derive the diagonal correlations of the Stokes fluctuations. The

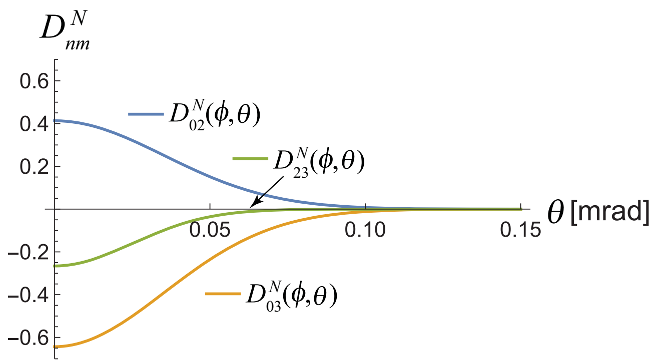

FIG. 4. Off-diagonal Stokes scintillations in the far zone as a function of the angle of observation θ. In this example $\phi = -1.0$ rad. The other parameters are the same as in Fig. 2.

results are

$$C^N_{00}(0,\theta) = \frac{1}{2}\exp[-k^2\theta^2(\sigma^2 - \Omega^2/2)]\left[\exp\left(-\frac{k^2\Omega^2\theta^2}{4}\right) + \alpha^4|B_{xy}|^2\exp\left(-\frac{k^2\Omega^2_{xy}\theta^2}{4}\right)\right], \quad (41a)$$

$$C^N_{11}(0,\theta) = \frac{1}{2}\exp[-k^2\theta^2(\sigma^2 - \Omega^2/2)]\left[\exp\left(-\frac{k^2\Omega^2\theta^2}{4}\right) - \alpha^4|B_{xy}|^2\exp\left(-\frac{k^2\Omega^2_{xy}\theta^2}{4}\right)\right], \quad (41b)$$

$$C^N_{22}(0,\theta) = \frac{1}{2}\exp[-k^2\theta^2(\sigma^2 - \Omega^2/2)]\left[\exp\left(-\frac{k^2\Omega^2\theta^2}{4}\right) + \alpha^4|B_{xy}|^2\cos(2\phi)\exp\left(-\frac{k^2\Omega^2_{xy}\theta^2}{4}\right)\right], \quad (41c)$$

$$C^N_{33}(0,\theta) = \frac{1}{2}\exp[-k^2\theta^2(\sigma^2 - \Omega^2/2)]\left[\exp\left(-\frac{k^2\Omega^2\theta^2}{4}\right) - \alpha^4|B_{xy}|^2\cos(2\phi)\exp\left(-\frac{k^2\Omega^2_{xy}\theta^2}{4}\right)\right]. \quad (41d)$$

It is easy to show, given the constraints on the source parameters as outlined in Sec. III, that these coefficients all decay exponentially as a function of the angle θ. The angular dependence of the four diagonal Stokes fluctuations coefficients is plotted in Fig. 5. The first coefficient, $C^N_{00}(0,\theta)$, represents the usual HBT effect (blue curve). Clearly, as can be seen from Eqs. (41a)–(41d), for our particular choice of a GSM beam, this coefficient is larger than the other three diagonal Stokes fluctuation correlations. As described above in Eq. (15), the sum of the these four coefficients is directly related to the modulus of the spectral degree of coherence $\eta(0,\theta)$. This quantity is therefore also plotted. It is seen that its angular half-width exceeds that of the four Stokes fluctuation correlations.

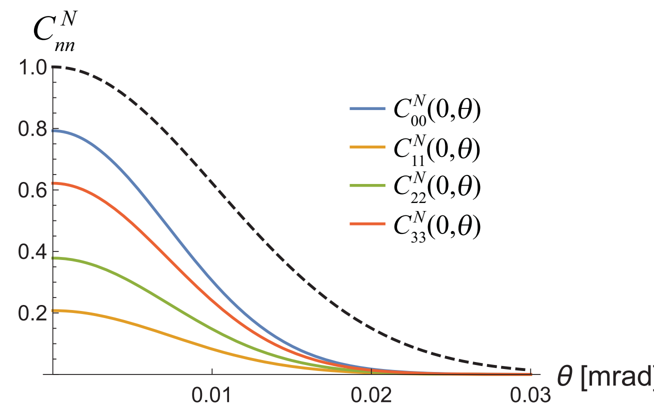

FIG. 5. The far-zone diagonal Stokes fluctuation coefficients $C^N_{nn}(0,\theta)$ as a function of the angle θ. The argument of the coefficient B_{xy} is taken to be $\phi = -1.0$ and the other parameters are the same as in Fig. 2. The dashed black curve indicates the modulus of the spectral degree of coherence $\eta(0,\theta)$. The curves at $\theta = 0$ represent, in descending order, $C^N_{00}(0,\theta)$, $C^N_{33}(0,\theta)$, $C^N_{22}(0,\theta)$, and $C^N_{11}(0,\theta)$.

A direct calculation shows that only six off-diagonal elements of the **C** matrix are nonzero, with only three of them being independent, namely

$$\begin{aligned} C^N_{02}(0,\theta) &= C^N_{20}(0,\theta) \\ &= \alpha^2\exp[-k^2\theta^2(\sigma^2 - \Omega^2/2)] \\ &\quad\times \exp\left[-k^2\theta^2\left(\Omega^2 + \Omega^2_{xy}\right)/8\right]|B_{xy}|\cos\phi, \end{aligned} \quad (42a)$$

$$\begin{aligned} C^N_{03}(0,\theta) &= C^N_{30}(0,\theta) \\ &= \alpha^2\exp[-k^2\theta^2(\sigma^2 - \Omega^2/2)] \\ &\quad\times \exp\left[-k^2\theta^2\left(\Omega^2 + \Omega^2_{xy}\right)/8\right]|B_{xy}|\sin\phi, \end{aligned} \quad (42b)$$

$$\begin{aligned} C^N_{23}(0,\theta) &= C^N_{32}(0,\theta) \\ &= \frac{1}{2}\alpha^4\exp[-k^2\theta^2(\sigma^2 - \Omega^2/2)] \\ &\quad\times \exp\left[-k^2\theta^2\Omega^2_{xy}/4\right]|B_{xy}|^2\sin(2\phi). \end{aligned} \quad (42c)$$

Not coincidentally, the nonzero off-diagonal elements of C^N_{nm} occur for the same values of n and m as those of the D^N_{nm} matrix. They also express the same functional dependence on the modulus of B_{xy} and its angle ϕ.

VI. CONCLUSIONS

Studies of the polarization properties of random electromagnetic beams, such as Refs. [14,17–19], have typically concentrated on the degree of polarization, the Hanbury Brown–Twiss effect, and scintillation. Recently the two concepts of the HBT effect and scintillation were generalized to so-called Stokes fluctuation correlations and Stokes scintillations. We examined the behavior of these 16 new quantities in the far zone of a random beam that is generated by a Gaussian Schell-model source. It was found that the different correlations and scintillations have varying spatial distributions, and that their dependence on the source parameters differs significantly. Our results also illustrate that these quantities may nontrivially depend on the average phase difference ϕ

between the two electric field components of the beam. For the specific model chosen here, for example, $D^N_{22}(\mathbf{r})$ and $D^N_{33}(\mathbf{r})$ vary sinusoidally with respect to ϕ, and the off-diagonal scintillation coefficients may be negative. Furthermore, the classical HBT coefficient is larger than the other three Stokes fluctuation correlation coefficients.

Our work shows that the HBT effect is just one of many correlations that occur in a random electromagnetic beam. These generalized HBT correlations can all be determined from intensity measurements and their values can then be used to characterize a beam in more detail than was previously done based on a single classical HBT measurement. They may also find application in inverse problems in which source parameters are reconstructed from far-zone observations.

ACKNOWLEDGMENT

This work is supported by the Air Force Office of Scientific Research under Award No. FA9550-16-1-0119.

[1] R. Hanbury Brown and R. Q. Twiss, A new type of interferometer for use in radio astronomy, Phil. Magazine **45**, 663 (1954).
[2] R. Hanbury Brown and R. Q. Twiss, Correlation between photons in two coherent beams of light, Nature (London) **177**, 27 (1956).
[3] R. Hanbury Brown, *The Intensity Interferometer* (Taylor and Francis, London, 1974).
[4] T. Shirai and E. Wolf, Correlations between intensity fluctuations in stochastic electromagnetic beams of any state of coherence and polarization, Opt. Commun. **272**, 289 (2007).
[5] T. Hassinen, J. Tervo, T. Setälä, and A. T. Friberg, Hanbury Brown–Twiss effect with electromagnetic waves, Opt. Express **19**, 15188 (2011).
[6] G. F. Wu and T. D. Visser, Correlation of intensity fluctuations in beams generated by quasihomogeneous sources, J. Opt. Soc. Am. A **31**, 2152 (2014).
[7] G. F. Wu and T. D. Visser, Hanbury Brown–Twiss effect with partially coherent electromagnetic beams, Opt. Lett. **39**, 2561 (2014).
[8] T. Shirai, Modern aspects of intensity interferometry with classical light, in *Progress in Optics*, edited by T. D. Visser (Elsevier, Amsterdam, 2017), Vol. 62, pp. 172.
[9] X. Liu, G. F. Wu, X. Pang, D. Kuebel, and T. D. Visser, Polarization and coherence in the Hanbury Brown–Twiss effect, J. Mod. Opt. **65**, 1437 (2018).
[10] D. Kuebel and T. D. Visser, Generalized Hanbury Brown–Twiss effect for Stokes parameters, J. Opt. Soc. Am. A **36**, 362 (2019).
[11] E. Wolf, *Introduction to the Theory of Coherence and Polarization of Light* (Cambridge University Press, Cambridge, 2007).
[12] M. Born and E. Wolf, *Principles of Optics*, 7th ed. (Cambridge University Press, Cambridge, 1999).
[13] L. C. Andrews and R. L. Phillips, *Laser Beam Propagation through Random Media*, 2nd ed. (SPIE, Bellingham, 2005).
[14] A. T. Friberg and T. D. Visser, Scintillation of electromagnetic beams generated by quasi-homogeneous sources, Opt. Commun. **335**, 82 (2015).
[15] F. Gori, M. Santarsiero, R. Borghi, and V. Ramírez-Sánchez, Realizability condition for electromagnetic Schell-model sources, J. Opt. Soc. Am. A **25**, 1016 (2008).
[16] O. Korotkova, M. Salem, and E. Wolf, Beam conditions for radiation generated by an electromagnetic Gaussian Schell-model source, Opt. Lett. **29**, 1173 (2004).
[17] D. F. V. James, Change of polarization of light beams on propagation in free space, J. Opt. Soc. Am. A **11**, 1641 (1994).
[18] O. Korotkova and E. Wolf, Changes in the state of polarization of a random electromagnetic beam on propagation, Opt. Commun. **246**, 35 (2005).
[19] O. Korotkova, T. D. Visser, and E. Wolf, Polarization properties of stochastic electromagnetic beams, Opt. Commun. **281**, 515 (2008).